# Field-dependent specific heat and magnetization for the S=12 antiferromagnetic chain Yb4As3: simulation and experiments

**G. Kamieniarz, R. Matysiak, Philipp Gegenwart, H. Aoki, A. Ochiai**

**Angaben zur Veröffentlichung / Publication details:**

Kamieniarz, G., R. Matysiak, Philipp Gegenwart, H. Aoki, and A. Ochiai. 2005. "Field-dependent specific heat and magnetization for the S=12 antiferromagnetic chain Yb4As3: simulation and experiments." *Journal of Magnetism and Magnetic Materials* 290-291: 353–56. https://doi.org/10.1016/j.jmmm.2004.11.259.

# Field-dependent specific heat and magnetization for the $S = \frac{1}{2}$ antiferromagnetic chain $Yb_4As_3$: simulation and experiments

G. Kamieniarz[a,*], R. Matysiak[b], P. Gegenwart[c], H. Aoki[d,1], A. Ochiai[d]

[a]*Computational Physics Division, Institute of Physics, A. Mickiewicz University, ul. Umultowska 85, Poznan 61-614, Poland*
[b]*Institute of Engineering and Computer Education, University of Zielona Góra, Poland*
[c]*Max Planck Instytute for the Chemical Physics of Solids, Dresden, Germany*
[d]*Center for Low Temperature Science, Tohoku University, Sendai 980-8578, Japan*

**Abstract**

The $S = \frac{1}{2}$ antiferromagnetic Heisenberg model with the transverse staggered field and uniform magnetic field perpendicular to the staggered field is applied to the semimetallic compound $Yb_4As_3$. The field-dependent specific heat for infinite and finite chains as well as the magnetization for infinite chains are calculated by the numerical quantum transfer-matrix method. Specific heat data for polydomain samples of $Yb_4As_3$ and $(Yb_{0.99}Lu_{0.01})_4As_3$ at $B = 12\,T$ are presented and compared with numerical results obtained for microscopic parameters taken from theoretical predictions. Magnetization data for single domain and polydomain samples of $Yb_4As_3$ are also compared with simulation results.

## 1. Introduction

The high-temperature phase of $Yb_4As_3$ is cubic with lattice constant $a = 8.788\,\text{Å}$ and has anti-$Th_3P_4$ crystal structure [1]. Above $T_{co} \approx 295\,K$ $Yb_4As_3$ is a homogeneous intermediate valence metal (IV) with a valence ratio of $Yb^{2+}/Yb^{3+} = 3:1$, where the Yb ions reside statistically on four equivalent families of chains along the space diagonals of a cube [1]. At $T_{co} \approx 295\,K$ the IV state exhibits such a charge-ordering instability that far below $T_{co}$ one of the four Yb ions becomes trivalent and forms a one-dimensional spin $S = \frac{1}{2}$ chain along the $\langle 1\,1\,1\rangle$ direction. The remaining Yb ions take non-magnetic divalent states. The crystal structure is trigonal with the angle 90.8° [1]. The $Yb^{3+}$ ion has one hole in the 4f closed shell. The $J = \frac{7}{2}$ ground multiplet splits into four doublets under the crystal field. Thus, the low-temperature dynamics is described by an effective $S = \frac{1}{2}$ spin chain. The neutron scattering experiments on $Yb_4As_3$ confirmed that the excitation spectrum is well described by the one-dimensional $S = \frac{1}{2}$ isotropic Heisenberg model [2] in the absence of magnetic field. The interchain interactions are small and ferromagnetic, leading to a low-$T$ spin-glass freezing [1]. On the other hand, the field-dependent data confirm the existence of a gap related to the Dzyaloshinskii–Moriya (DM)

*Corresponding author. Tel.: +48 61 8295071; fax: +48 61 8257758.
*E-mail address:* gjk@amu.edu.pl (G. Kamieniarz).
[1]Present address: Tokyo University, Institute for Solid State Physics, Kashiwa, Chiba 2708581, Japan.

interaction [3] which can be mapped onto the anisotropic Heisenberg model with both uniform field $B^x$ and staggered field $B_s^y$ [4].

Below we also focus on $(Yb_{0.99}Lu_{0.01})_4As_3$. The nonmagnetic Lu-atoms are randomly distributed over all different Yb sites—both on the magnetic chain and on the nonmagnetic chains. The partial substitution of Yb with nonmagnetic Lu-atoms effectively dilutes the magnetic $S = \frac{1}{2}$ chain by the introduction of nonmagnetic static defects [5] and should affect the field-dependent specific heat behaviour.

## 2. Model and simulation technique

To characterize the finite-temperature properties of the $Yb_4As_3$, we consider the $S = \frac{1}{2}$ Heisenberg model with the DM interaction [4,6]. The DM interaction is eliminated by rotating the spins in the $x - y$ plane by the angle $\theta$ [4]. Then the model is mapped onto

$$\mathscr{H} = -J\sum_{i=1}^{N}\mathbf{S}_i\mathbf{S}_{i+1} - g_\perp\mu_B B^x\sum_{i=1}^{N}S_i^x - g_\perp\mu_B B_s^y\sum_{i=1}^{N}(-1)^i S_i^y, \quad (1)$$

where $B^x = B\cos(\theta)$, $B_s^y = B\sin(\theta)$ and $B$ is the uniform external magnetic field perpendicular to the one-dimensional spin-chain. Eq. (1) describes the effective isotropic Heisenberg model with both the uniform field $B^x$ and the transverse staggered field $B_s^y$. We apply the quantum transfer-matrix (QTM) simulation technique. Following the scheme for infinite chains described in Ref. [6], we have calculated the partition function from the largest eigenvalue of the global transfer-matrix.

For finite chains we have applied the vectors $|a\rangle$ and $\langle b|$ described in Ref. [7] and we have used the following equations to calculate the $m$th classical approximant to the partition function of Eq. (1).

$$Z_m = \langle b|(W_1W_2)^{(N-1)/2}|a\rangle \quad \text{for} \quad \text{odd } N, \quad (2)$$

$$Z_m = \langle b|(W_1W_2)^{N/2-1}|a\rangle \quad \text{for} \quad \text{even } N. \quad (3)$$

We have tested our simulations for the finite chains using the results obtained from the exact diagonalization technique for the limit $B = 0$ [8]. In Fig. 1 we present the quantum transfer-matrix results for the finite chains (open symbols) as a function of $1/m^2$. The exact diagonalization data (full symbols) for $N = 8$ and 15 stand for the expected limit of our approximants when $m \to \infty$. For the macroscopic chains, the convergence is similar but deteriorates down to 5% for $B \neq 0$ in (1) and $k_BT/J \approx 0.15$.

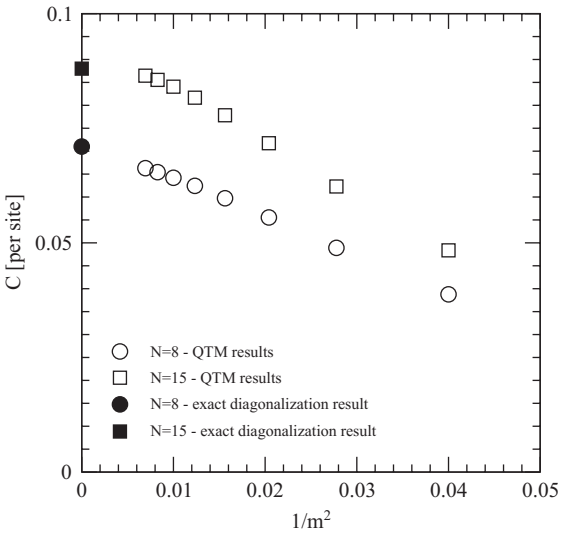


Fig. 1. Variation of the zero-field specific heat per spin at $k_BT/J = 0.05$ against $1/m^2$ for the finite-chain QTM results ($m = 5, \ldots, 12$). Full symbols represent the exact diagonalization data.

## 3. Experimental results and numerical data

The experiments were carried out on high-quality single crystals of $(Yb_{1-x}Lu_x)_4As_3$ prepared as described in Refs. [5,9]. For the specific heat measurements a microcalorimeter from Oxford Instruments was used. The transfer-matrix simulations of the specific heat and magnetization were performed using the parameters: $g_\parallel = 2.9$, $g_\perp = 1.3$ [10], $J/k_B = -26\,\text{K}$ [2] and $\tan(\theta) = 0.19$ [4].

The specific heat results obtained in the magnetic fields from extrapolations of the largest eigenvalues of the transfer matrices ($4 \leqslant m \leqslant 12$, $N$ infinite), are presented in Fig. 2. The uncertainties are smaller than the size of the symbols at higher temperatures and reach the size of the symbols near $T = 4\,\text{K}$. The open symbols represent our experimental results for a polydomain sample with the magnetic field applied along the cubic $\langle 1\,1\,1\rangle$ direction [3] and the remaining symbols are numerical results. For the experimental data the phonon contribution $C_{ph} = 2.05 \times 10^{-3}\,T^3\,\text{J}/(\text{K}^4\,\text{mol})$ has been subtracted [3]. The computer calculations were performed for a polydomain sample in which 25% of the domains were oriented with the spin chains parallel to the applied field $B$ and about 75 of the domains were aligned so that the effective field component $B\sin(70^\circ)$ was perpendicular to the spin chains. With increasing magnetic field the maximum in specific heat divided by temperature increases, shifts to the right and the $C/T$ curves intersect at about 9 K, which is consistent with the experimental findings.

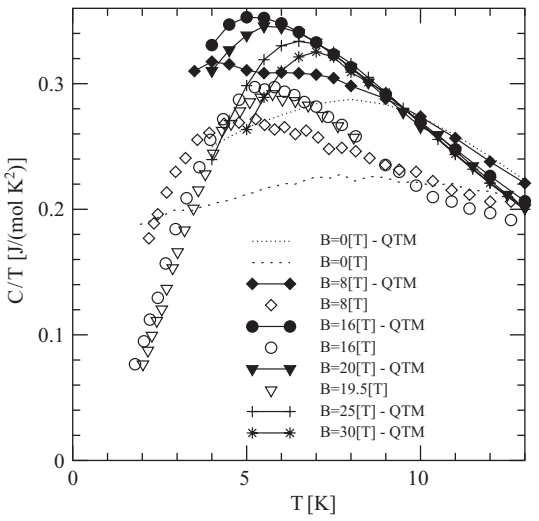


Fig. 2. Comparison of the QTM results and the measured specific heat for $Yb_4As_3$ after phonon subtraction.

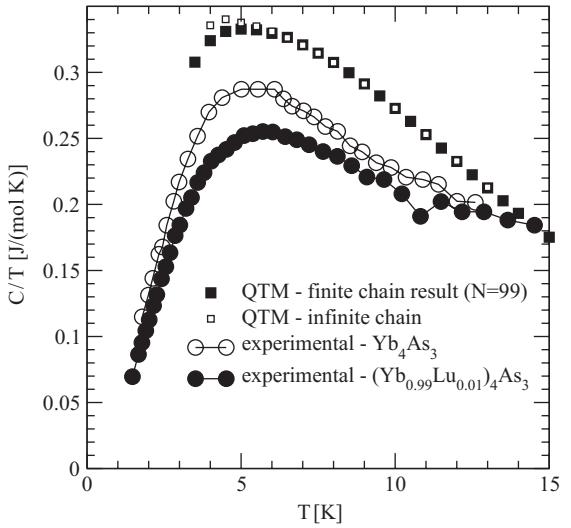


Fig. 3. Comparison of the QTM results (square symbols) and polydomian specific heat for $Yb_4As_3$ and $Yb_{0.99}Lu_{0.01})_4As_3$ (Circle symbols).

Similar behaviour we have recovered for the 1% diluted system. In Fig. 3, using Eqs. (2) and (3) we have compared specific heat experimental results for a polydomain $(Yb_{0.99}Lu_{0.01})_4As_3$ sample in the applied field $B = 12\,\mathrm{T}$ and numerical data for the finite $N = 99$ chain. We expect that the reduction of the specific heat will be stronger when the distribution of chain segments is taken into account in the simulations. Our theoretical specific-heat data systematically overestimate the experimental results. This has not been understood so far.

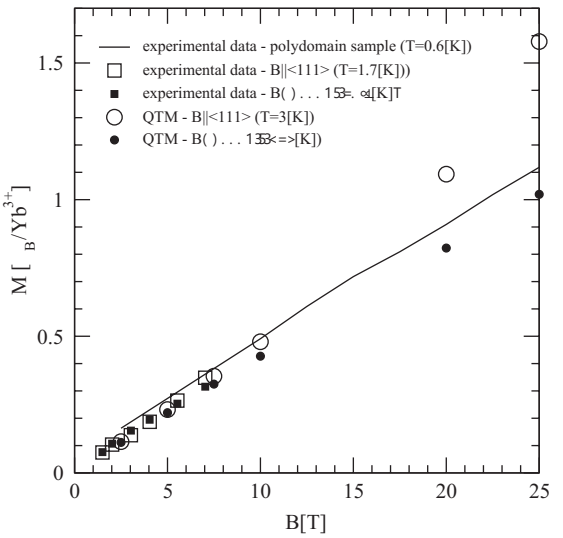


Fig. 4. The field-dependent magnetization for $Yb_4As_3$: experimental data (single domain and polydomain sample) and numerical data.

We have also analysed the magnetization data. To achieve the convergence of our extrapolations up to $B = 25\,\mathrm{T}$, we performed simulations of the field-dependent magnetization at $T = 3\,\mathrm{K}$. In Fig. 4 we present these results for the field perpendicular and parallel to the chains (full and open circles, respectively), where vanVleck-type ($\chi_\perp = 0.0324$ and $\chi_\parallel = 0.0205$) contributions [10] are added. We also plot the experimental data obtained at 0.6 K for a polydomain sample [3] by continues line. Single-domain magnetization results [10] for $T = 1.5\,\mathrm{K}$ and 1.7 K for the field perpendicular and parallel to the chains, respectively, are represented by squares. Our estimates in the low-field limit are consistent with experiment and the DMRG calculations [10].

## 4. Conclusions

We have presented experimental data of field-dependent specific heat and magnetization measurements. The former refer both to the pure and diluted system. We have successfully compared them with quantum transfer-matrix calculations performed for the Heisenberg model with the DM interactions, revealing at least a qualitative agreement with the experiments.

## Acknowledgements

We thank Dr. B. Schmidt and Dr. P. Thalmeier for helpful discussions, the Committee for Scientific

Research—for a partial support via the grant 4 T11F 014 24 and PSNC—for an access to the supercomputing platforms.

## References

[1] B. Schmidt, et al., Physica B 300 (2001) 121.
[2] M. Kohgi, et al., Phys. Rev. B 56 (1997) R11388.
[3] P. Gegenwart, et al., Physica B 312–313 (2002) 315.
[4] N. Shibata, et al., J. Phys. Soc. Japan 70 (2001) 3690.
[5] A. Ochiai, et al., Jpn. J. Appl. Phys. Ser. 11 (1999) 117.
[6] R. Matysiak, et al., Phys. Stat. Sol. (b) 237 (2003) 549.
[7] T. Delica, H. Leshke, Physica A 168 (1990) 736.
[8] G. Kamieniarz, et al., Phys. Rev. E 56 (1997) 144.
[9] A. Ochiai, et al., J. Phys. Soc. Japan 59 (1990) 4129.
[10] K. Iwasa, et al., Phys. Rev. B 65 (2002) 052408.